Shared Neural Substrates Support Seasonal, Developmental, and Evolutionary Shifts in Sensorimotor Integration

Authors: Martin W. Jarzyna[1], Bruce A. Carlson[1*]

Affiliations: [1] Department of Biology, Washington University, St. Louis, MO 63130-4899

* Corresponding Author: Bruce A. Carlson (carlson.bruce@wustl.edu)

ORCID:
Martin W. Jarzyna (0000-0002-2485-6589)

Bruce A. Carlson (0000-0002-2151-0443)

Author Contributions
M.W.J. and B.A.C. designed research; M.W.J. performed research; M.W.J. analyzed data; M.W.J. and B.A.C. wrote the manuscript.

Competing Interest Statement
The authors declare no competing interest.

Classification
Neuroscience

Keywords
Sensorimotor integration, Electrosensory system, Neurophysiology, Plasticity, Neuroendocrinology, Evolution, Neurodevelopment, Neuroethology

Acknowledgment
This work was supported by the National Science Foundation (IOS-2203122 to B.A.C.) and the National Institutes of Health (F31NS139904 to M.W.J.). We thank Matasaburo Fukutomi for collecting data for Figure S1 and for assistance with hormone treatment protocols. We thank Dr. Martha Bagnall for comments on the manuscript.

Summary
Nervous system function depends on accurate predictions of the sensory consequences of one's own actions. Internal copies of motor commands, termed corollary discharge (CD), modulate activity in

sensory neurons to discriminate between self-generated sensory input (reafference) and externally generated inputs (exafference). As behavior changes through development and evolution, these predictions must be updated to account for resulting changes to reafference. However, the mechanisms that synchronize CD to reafferent input remain unknown. We addressed this question using mormyrid fish. Mormyrids communicate using electric organ discharges (EODs), and electroreceptors specialized for communication respond to both reafferent and exafferent EODs. To block responses to reafferent EODs, a CD briefly inhibits central electrosensory neurons each time an EOD is produced. EOD duration is diverse both across and within species, and CD timing has evolved to maintain a precise match between the timing of inhibition and reafferent sensory input. Similarly, seasonal increases in testosterone reversibly elongate male EODs in some species, and testosterone shifts CD timing in the brain to match the resulting shift in reafferent feedback. Here, we identify neural substrates for seasonal, developmental, and evolutionary shifts in the timing of CD activity within this circuit. We treated *Brienomyrus brachyistius* with testosterone to elongate EODs and induce CD plasticity, then recorded field potentials from six nuclei linking electromotor, CD, and electrosensory pathways. Testosterone delayed synaptic input and elongated field potentials in the mesencephalic command-associated nucleus (MCA) of the CD pathway, which shifted downstream activity. We recorded from these same areas in two species of *Campylomormyrus* with dramatically different baseline EOD durations: one with short-duration EODs (~0.2 ms), and one with long EODs that displays pronounced developmental plasticity of EOD duration (2-26 ms). Long-EOD fish also had delayed and elongated MCA activity relative to short-EOD fish, and these shifts again propagated through the circuit. Our results reveal that distinct processes—hormonal plasticity operating over days, developmental changes unfolding over years, and evolutionary divergence over millions of years—converge on the same neural substrates to synchronize CD with reafferent input. This suggests that sensorimotor systems can evolve a common solution for temporal coordination across timescales.

Introduction

Correctly attributing a sensory input as self- or externally generated can be a matter of life and death: Consider the sound of rustling leaves, which could arise from one's own footsteps or those of a rapidly approaching predator. Because peripheral receptors cannot distinguish self-generated (reafferent) from externally generated (exafferent) stimuli, motor areas send copies of motor commands called corollary discharge (CD) to sensory neurons[1,2]. In response to CD input, sensory neurons adjust their responses to stimuli to account for the reafferent input predicted to arise from an animal's own behavior[3–5]. However, neither behavior nor neural circuits are static—both change over ontogenetic and evolutionary timescales in response to environmental demands. Much of this behavioral diversity, from reversible seasonal changes to evolutionary divergence across lineages, arises from correlated modifications to the physiology of motor effectors, sensory receptors, and central circuits[6–11]. However, we lack mechanistic understanding of how these parallel changes are coordinated to coherently reshape behavior. How do CD circuits maintain accurate motor representations during these transitions? CD signals require precise temporal regulation to accurately predict reafferent input, yet the mechanisms that preserve this precision as behavior changes are unknown. Further, do nervous systems evolve unique solutions to mediate developmental plasticity versus evolutionary change, or are the same substrates "reused" regardless of the timescale over which behavior changes? This study investigates these questions using a well-known CD circuit in mormyrid weakly electric fish.

Mormyrids generate electric fields called electric organ discharges (EOD) for communication and electrolocation. Because these fields do not propagate as waves, unlike acoustic signals, the temporal structure of electric signals is preserved during signal transmission[12]. This permits mormyrids to communicate behaviorally relevant information with submillisecond resolution. The EOD waveform is stereotyped and encodes the sender's identity through species, sex, and social status

differences[13,14]. EOD waveform is determined by the morphophysiological characteristics of electrocytes, the excitable cells of the electric organ near the tail[14]. Each EOD is initiated by a hindbrain Command Nucleus (CN)[14].

Mormyrids process electric communication signals through a dedicated pathway[15,16]. Electroreceptors in the skin called knollenorgans (KO) respond to a fish's own EODs, as well as those of other fish, with short latency, time-locked spikes[13]. KOs relay these spikes to the nucleus of the electrosensory lateral line lobe (nELL) in the hindbrain, which also receives inhibitory input from an electric organ corollary discharge pathway (CD)[17]. The CD pathway is activated by the CN that also controls EOD production, and consists of a chain of two excitatory nuclei (the bulbar- and mesencephalic command-associated nuclei [BCA and MCA]) followed by a sublemniscal nucleus (slem) that inhibits nELL neurons when they are excited by reafferent stimuli[17,18] (Figure 1A). Due to this precisely timed inhibition, downstream electrosensory neurons selectively process signals from other fish[16].

Across mormyrid species, EOD waveforms have diversified extensively and vary from hundreds of microseconds to tens of milliseconds in duration[19,20]. Due to their biophysical properties, KO receptors produce a short-latency spike following the first peak of each reafferent EOD[21–23]. As such, fish with long EODs experience delayed sensory input from their own EODs compared to fish with short EODs[21,24]. Recent comparative work showed that CD inhibition of nELL is tightly coupled to the timing of reafferent input, such that long-EOD species exhibit delayed CD inhibition compared to short-EOD species[21]. This relationship also holds intraspecifically in individuals of *Campylomormyrus numenius,* whose EODs can increase in duration throughout ontogeny from 1-2 ms in juveniles to >20 ms in adults[20,21]. This suggests that internal delays shift the timing of CD inhibition in the brain to optimally block reafferent stimuli (Figure 1C)**.** As EOD duration is determined peripherally in the electric organ, it is unclear how a precise match in timing evolved between EOD duration and CD signals, and how this is maintained during development.

In addition to varying across species, EOD duration and CD timing can undergo reversible plasticity in response to steroid hormones. During the breeding season, sexually mature males of some species develop longer EODs than females[25]. This sex difference arises when heavy rainfall decreases conductivity of mormyrid habitats, which acts as a cue to increase gonadal steroid hormone production[26]. Steroids act directly on electrocytes and induce biophysical changes that elongate EODs[27–30]. Exogenous testosterone (T) treatment elongates EODs in juveniles, females, and non-breeding males, indicating that seasonal sex differences are due to activational effects of hormones, and are not inherent to male or female electric organs[25]. A recent study found that T-induced EOD elongation delays activation of KO receptors, thus reversibly shifting the timing of reafferent feedback[22]. To match this shift in reafference, T acts directly in the brain, independent of sensory feedback, to shift CD inhibition timing (Figure 1D)[22]. These results provide evidence for coordinated hormonal effects in the periphery and in central CD circuitry to maintain self/other recognition during behavioral plasticity.

To date, shifts in CD timing have only been measured indirectly within the KO sensory pathway in the exterolateral nucleus (EL), which receives input from nELL neurons[21,22]. Thus, the neural substrates underlying seasonal, developmental, and evolutionary shifts within the CD circuit are unknown. In this study, using extracellular field potential recordings, we determine the neural substrate for T-induced shifts to CD inhibition. We then determined the substrate of interspecific and inter-individual differences in CD by comparing the timing and waveforms of CD activity in naturally short- and long-EOD species. Our results demonstrate that shared neural substrates maintain a precise link between reafferent sensory input and corollary discharge across multiple timescales of behavioral change.

Results

Testosterone shifts CD timing in the mesencephalic command-associated nucleus (MCA)

We first treated *Brienomyrus brachyistius* with 17-α methyltestosterone (T) for 2 weeks, according to a previous study[22] (n=4 each group, see Methods). We recorded EODs of freely swimming fish before and after hormone treatment. As expected, T-treated fish showed a nearly 3-fold elongation of EOD duration compared to vehicle (V [all values reported as mean ± standard deviation]: 0.43±0.04 ms, T: 1.13±0.04 ms; t_6=-25.6, p<1 x 10^{-6}, Student's *t*-test). Unexpectedly, V-treated fish experienced a slight but statistically significant elongation of EODs (V pre-treatment: 0.36±0.02 ms, V post-treatment: 0.43±0.04 ms, t_3=-5.6, p<0.05, paired Student's *t*-test). While V treatment was associated with a small shift to reafferent timing, we note that the change in EOD duration had an effect size that was 11.8x stronger in T compared to V fish (Cohen's *d*=25.1 for T and 2.1 for V).

The EOD elongation induced by this time course of T treatment delays reafferent input to KOs. Concurrently, T both delays onset of CD inhibition and elongates the CD inhibition window[22]. To determine where in the CD pathway this shift in timing arises, we sequentially recorded extracellular EOD command-related field potentials from each nucleus along the pathway, from CN to nELL (CN, MRN, BCA, MCA, slem, nELL; Figure 1). To our knowledge, this is the first time these areas have all been recorded from within the same individuals. CD nuclei exhibit synchronized activity time-locked to EOD production, reflected in stereotyped waveforms of their field potentials[17,31,32]. These potentials occur at a characteristic latency relative to EOD production, with latency increasing at each step in the pathway. In our preparation, neuromuscular paralysis silences the electric organ, but spontaneous activation of the electromotor and CD pathways continues. The EOD command (EODC) can be recorded from spinal electromotor neurons that normally activate the electric organ using an electrode pair placed near the tail, giving a reliable fictive EOD signal[14,33]. The EODC was thus a reference to determine whether T alters the timing of command-related activity at a given point in the pathway. As CD nuclei receive no known external inputs and exhibit no spontaneous activity in the absence of CN input, field potentials recorded from this simple excitatory relay are exclusively CD-related[31,32].

To determine hormonal effects on the CD pathway, we compared timing between T- and V-treated fish at each nucleus in terms of latency of the first peak of the field potential relative to the EODC (termed "onset"), and the time between first and last peak of the field potential (termed "duration"). Though relative amplitude and polarity of field potentials depended on electrode position relative to nuclei, field potential timing was stable for each fish regardless of amplitude and polarity. In CN, which issues the central command to activate the electric organ and the associated CD, we observed no significant differences between groups in onset (Figure 2; V: -2.26±0.16 ms, T: -2.16±0.25 ms; t_5=-0.66, p=0.54, Welch's *t*-test) or duration (V: 3.10±0.36 ms, T: 2.85±0.40 ms; t_5=0.92, p=0.39). CN issues the electromotor command via short-latency activation of the medullary relay nucleus (MRN). We also observed no significant differences in MRN onset (V: -2.05±0.06 ms, T: -1.98±0.24 ms; t_3=-0.59, p=0.6) or duration (V: 2.10±0.12 ms, T: 1.90±0.15 ms; t_4=1.83, p=0.14).

In the CD pathway, we observed no significant differences after T treatment in BCA onset (V: -2.03±0.20 ms, T: -1.87±0.27 ms; t_5=-0.98, p=0.37) or duration (V: 2.24±0.06 ms, T: 2.07±0.25 ms; t_3=1.3, p=0.28). However, MCA onset was significantly delayed in T-treated fish compared to vehicle (V: -1.20±0.07 ms, T: -0.78±0.17 ms; t_4=-4.71, p<0.01), and this delay continued through slem (V: 0.04±0.09 ms, T: 0.47±0.13 ms; t_5=-5.4, p<0.01) and nELL (V: 3.6±0.42 ms, T: 4.57±0.49 ms; t_6=-3.1, p<0.05).

In addition to CD delays, we observed significant elongation after T treatment in field potential waveforms of MCA (V: 2.95±0.20 ms, T: 3.73±0.38 ms; t_5=-3.6, p<0.05) and slem (V: 0.76±0.05 ms, T: 2.04±0.10 ms; t_6=-23, p=2.1 x 10^{-5}). These elongations were typically accompanied by an additional peak in the waveforms of T-treated fish compared to vehicle, which was clearly visible in

MCA potentials from 3 of 4 T-treated fish, and in slem potentials from all 4 T-treated fish (Figure 2). Together, our results show that MCA is the likely origin of the CD inhibition shifts previously observed in downstream electrosensory neurons of T-treated fish.

Species differences in CD timing originate in the mesencephalic command-associated nucleus (MCA)

We next sought to determine the neural substrate of species differences in CD timing. We first compared electrosensory data from a past study on two species of *Campylomormyrus* that differ in EOD duration[21]. *Campylomormyrus compressirostris* ("*C. com*") had short EODs that were similar between individuals, whereas *Campylomormyrus numenius* ("*C. num*") possessed longer EODs whose duration varied extensively across individuals. Though this study investigated how CD timing varied across seven mormyrid species, it did not directly compare the kinetics of CD timing in these two *Campylomormyrus* species[21]. Compared to short-EOD *C. com*, CD inhibition in long-EOD *C. num* was both delayed in its onset (Figure S1A; *C. com*: 2.50±0.10 ms, *C. num*: 3.74±0.40 ms; t_6=-7.2, p<0.001) and elongated (Figure S1B; *C. com*: 1.89±0.07 ms, *C. num*: 2.83±0.51 ms; t_5=-4.4, p<0.01). Importantly, these differences precisely matched species differences in the timing of reafferent input (for more details on recording, see[21]). This natural variation provided an excellent system in which to test whether evolutionary changes to the EOD shift inhibition by acting on the same components of the CD circuit as T-induced seasonal changes.

We performed similar recordings of command-related potentials throughout the CD pathway in *C. com* (EOD duration: 0.147±0.004 ms for 5 individuals with EOD data, 8 individuals total) and *C. num* (2.478±0.414 ms, n=7). To our knowledge, these were the first recordings of electromotor or CD pathways from any *Campylomormyrus* species. We observed no interspecific differences in onset timing of CN (Figure 3; *C. com*: -2.05±0.21 ms, *C. num*: -2.08±0.12 ms; t_{10}=0.38, p=0.71). Duration of CN field potentials was also similar between species (*C. com*: 2.86±0.44 ms, *C. num*: 2.95±0.32 ms; t_9=-0.46, p=0.66). We also observed no differences in onset or duration between species in MRN (Onset: *C. com*: -1.93±0.16 ms, *C. num*: -1.97±0.15 ms; t_{12}=0.52, p=0.62; Duration: *C. com*: 1.90±0.08 ms, *C. num*: 1.97±0.04 ms; t_8=-0.93, p=0.38) or in BCA (Onset: *C. com*: -1.94±0.19 ms, *C. num*: -1.95±0.12 ms, t_{12}=0.10, p=0.92; Duration: *C. com*: 1.99±0.14 ms, *C. num*: 2.10±0.11 ms; t_{12}=-1.7, p=0.11).

As in T-treated fish, we found a significant delay to the onset of MCA in long-EOD *C. num* compared to short-EOD *C. com* (*C. com*: -1.18±0.14 ms, *C. num*: -0.91±0.13 ms; t_{13}=-3.9, p<0.01). Again, the delay originating at MCA carried through to slem (*C. com*: 0.12±0.13 ms, *C. num*: 0.58±0.07 ms; t_{11}= -8.5, p=3.6 x 10^{-6}) and nELL (*C. com*: 4.29±0.16 ms, *C. num*: 5.61±0.42 ms; t_8=-7.9, p=4.9 x 10^{-5}). Compared to *C. com*, *C. num* also had elongated field potentials in MCA (*C. com*: 2.42±0.08 ms, *C. num*: 3.17±0.4 ms; t_6=-4.6, p<0.01) and slem (*C. com*: 0.89±0.04 ms, *C. num*: 2.02±0.15 ms; t_7 = -18.8, p=2.9 x 10^{-7}). In summary, a long-EOD *Campylomormyrus* species showed both delayed and elongated activity in MCA and slem compared to a short-EOD species, and these shifts delayed inhibition of nELL.

CD onset and duration correlate with reafference downstream from the bulbar command-associated nucleus (BCA)

Remarkably, we observed species differences in the same loci as those in which hormonal plasticity occurred. To determine how these shifts in the brain relate to the reafferent input experienced by these fish, we performed simultaneous recordings of the EOD and EODC prior to our field potential recordings. By convention, we recorded EODs with the recording electrode near the head and the reference electrode near the tail, which results in a head-positive waveform. Reafferent input to KO receptors corresponds nearly 1:1 with the first head-positive peak of the EOD[21,22]. We thus quantify this estimated reafferent timing as the delay from the EODC to EOD peak 1, which we term

"reafferent delay" (Figure 4G). We measured the correlation between timing of CD onset and reafferent delay, and between field potential duration and reafferent delay, across the four groups tested (V- and T-treated *B. brachyistius*, *C. com*, and *C. num*). We computed linear regressions and found no significant relationship between onset timing or duration and reafferent delay in CN (Figure 4A; onset: r^2=0.001, p=0.89; duration: r^2=0.002, p=0.84), MRN (Figure 4B; onset: $r^2=3.56 \times 10^{-6}$, p=0.99; duration: r^2=0.010 , p=0.68), or BCA (Figure 4C; onset: $r^2=6.7 \times 10^{-5}$, p=0.97; duration: r^2=0.011, p=0.67) . However, we found that both CD onset and duration significantly correlated with reafferent delay in MCA (Figure 4D; onset: r^2=0.37, p<0.01; duration: r^2=0.29, p<0.05) and slem (Figure 4E; onset: r^2=0.48, p<0.001; duration: $r^2=0.75$, $p=7.5 \times 10^{-7}$). We note that slem duration showed a stark bimodal separation between short- and long-EOD groups. Lastly, nELL onset correlated strongly with reafferent delay (Figure 4F; r^2=0.62, $p=3.0 \times 10^{-5}$).

Long-term developmental shifts to CD also arise in MCA

In addition to the reversible elongation induced by T, EOD duration can progressively increase throughout ontogeny in some species. Some individuals of *C. numenius* develop particularly long EODs in adulthood, reaching durations of tens of milliseconds[20]. We obtained a single individual of *C. numenius* with a 26.1 ms EOD (>10x the mean duration of the *C. num* above), from which we performed similar recordings. While rigorous characterization of CD plasticity across development is not possible with a single individual, we compared this extreme exemplar to shorter-EOD conspecifics to test whether common substrates also support ontogenetic changes in CD timing.

Simultaneous EOD/EODC recordings revealed that this fish experienced reafference at a delay of 8.16ms, roughly 4.6 ms later than in the other conspecific *C. num* we measured (Figure 5A). Onset of CN, MRN, and BCA all occurred at similar latencies in this superlong-EOD fish compared to conspecifics (Figure 5C; CN [all presented as onset time, Z score relative to mean *C. num* onset, and p(onset < -Z or onset > Z)] : -1.98 ms, Z=0.86, p=0.39; MRN: -1.91 ms, Z=0.37, p=0.71; BCA: -1.84 ms, Z=0.87, p=0.39). We observed a remarkable delay in the pathway beginning at the onset of MCA (onset=4.17 ms, Z=39.4, $p < 1 \times 10^{-10}$), and this again carried through to slem (onset=6.48 ms, Z=64.6, $p < 1 \times 10^{-10}$) and nELL (onset=11.58 ms, Z=14.38, $p < 1 \times 10^{-10}$). We note that the final timing of nELL field potentials closely matched the nearly 5 millisecond difference in expected reafferent input experienced by the fish, underscoring the precision of CD delays occurring downstream from MCA.

Durations scaled more variably than onset timing in the superlong-EOD fish compared to conspecifics. CN and MRN durations were comparable to shorter-EOD conspecifics (CN duration=3.45 ms, Z=1.54, p=0.12; MRN duration=1.68 ms, Z=-1.54, p=0.12). Unexpectedly, durations were shorter than conspecific *C. numenius* in BCA (duration=1.77 ms, Z=-3.01, p<0.01), and trended shorter, to a lesser degree, in MCA (duration=2.33 ms, Z=-1.95, p=0.051). Slem duration was comparable to conspecifics (duration=2.23 ms, Z=1.4, p=0.16). In summary, ontogenetic EOD elongation was associated with extreme CD delays in the same loci as seasonal and evolutionary changes, whereas field potential durations were generally species-typical.

Discussion

Our results show that a shared neural substrate supports reversible hormonal plasticity, long-term developmental plasticity, and evolutionary change of corollary discharge (CD) timing in mormyrid fish. CD shifts enable fish to maintain accurate reafferent cancellation as their own communication signals change throughout lifetime and diversify over evolutionary time. We found that changes to CD consistently stemmed from differences in onset and duration of MCA activity, and these differences propagated through the GABAergic slem and electrosensory nELL. This preserves the temporal relationship between behavior and resultant sensory feedback through different states. The convergence of neural substrates across timescales suggests that mormyrid brains evolved a robust solution for correcting prediction errors in neural circuits, regardless of the mechanism driving the

error. This may reflect a fundamental principle for temporal coding across sensorimotor systems: inducing shifts at a single well-tuned node as opposed to multiple independent loci could be metabolically efficient and ensure coherent output. This may be especially important in systems where temporal precision is paramount, such as sound localization and echolocation circuitry. Notably, we observed no differences in timing within the electromotor command pathway (CN, MRN, BCA) across groups. This result aligns with previous evidence that changes in the EOD waveform are not associated with any changes to the EOD command, suggesting that changes to EOD waveform are exclusively due to biophysical effects on the electric organ[25,33].

The delay to nELL potentials scaled steadily with reafference, exhibited most dramatically in a superlong-EOD *C. numenius*[21,24]. These fine-tuned delays allow CD inhibition to coincide with reafferent input to nELL from knollenorgan primary afferents, which is triggered by inward currents across the skin[24]. For self-generated EODs, this occurs shortly after the first head-positive EOD peak[21,22]. Curiously, field potential durations showed a more categorical change across groups, with a single additional peak often visible in the waveforms of MCA and slem in T-treated fish and *C. numenius* compared to V-treated fish and *C. compressirostris*. Unlike the long delays observed in superlong-EOD *C. numenius*, field potential durations were comparable to conspecifics. Elongated inhibition likely allows the system to cover additional knollenorgan spikes elicited by longer EODs, as observed after T-treatment recently by Fukutomi & Carlson[22]. That delays scaled continuously while durations shifted more categorically and plateaued suggests that these two changes may have distinct physiological bases. In any case, these shifts likely balance the need for effective blocking of reafferent input as EODs elongate, while minimizing the resultant period of insensitivity.

CD delays likely originate at inputs to the mesencephalic command-associated nucleus (MCA)

What neuronal activity do these shifts represent? The complex field potentials recorded near MCA are thought to reflect a mixture of presynaptic activity from BCA axon terminals and postsynaptic MCA neurons[34]. Past intracellular and extracellular recordings by Bell et al. suggest that BCA axons contribute the first and last peaks in the waveform, while the two inner peaks arise from MCA neurons[34]. In T-treated fish and *C. numenius*, we observed delayed onset of the entire field potential, as well as consistent elongation of the time between the first and last peaks with an additional peak in many cases. Because these putative pre- and postsynaptic elements were challenging to fully separate without using intra- or juxtacellular recordings, it is unclear whether the additional peak represents extra activity in BCA axons or MCA neurons. While future intracellular recordings will seek to definitively determine the cellular origin of these changes, our data suggest that neuronal excitability is modified at one or more sites. A major possibility is that delayed MCA activation in long-EOD fish originates in BCA: Since activity at BCA terminals is delayed while potentials near BCA somas are unaffected in long-EOD fish, delays may accumulate in the long axonal projection from BCA to MCA, and/or at BCA-MCA synapses. Elongations to MCA potentials could originate from altered presynaptic input from BCA and/or altered postsynaptic responses in MCA. Whatever their basis, these shifts drive corresponding changes in slem, where an additional peak was observed in all long-EOD fish. It is unclear whether these waveform changes also involve physiological remodeling of slem, or if they are passively carried from MCA onward.

Putative physiological basis of CD shifts

CD delays could arise via several mechanisms in the long projection from BCA to MCA. Elongation of BCA axons in long-EOD fish would delay the signal's arrival at axon terminals, reminiscent of delay lines observed in many systems where temporal information must be tightly preserved[35–38]. Such a mechanism is plausible over long-term development, and over shorter timescales given neurotrophic effects of androgens on neurite outgrowth[39,40]. Conduction velocity can also be lowered by decreasing axon diameter via cytoskeletal remodeling or reduced myelin thickness[41,42]. A third possibility is altered Ranvier node composition and/or internode distance, which can be separately

tuned within the same axon to control action potential propagation speeds[43]. Indeed, adjustments to internode distance and the presence of specialized inexcitable nodes allows the South American electric fish *Stenarchus* to maintain synchronous activation of its electric organ despite varying axonal length from the pacemaker nucleus that controls EOD production[44,45]. Similar specializations in mormyrid brains may underlie the remarkable range of delays observed between BCA and MCA field potentials.

Shifts to CD may also accumulate at BCA-MCA synapses. Steroid hormones affect virtually all known voltage-dependent conductances and neurotransmitter receptors, so possibilities are numerous[46]. Hormonal effects on voltage-gated Ca^{2+}channels could alter kinetics of neurotransmitter release to delay or elongate presynaptic input from BCA[47]. These effects could also be mediated postsynaptically in MCA through regulation of AMPA receptors or their subunits. The additional spike observed in MCA and slem waveforms may be akin to burst firing from afterdepolarizations. If altered currents generate sufficient afterdepolarizations, such as those generated by R/T type Ca^{2+} currents, or persistent/resurgent Na^{+} currents, an additional spike could be elicited each time a CD input arrives[48]. A combined physiological and morphological approach will be necessary to determine the source of these temporal coding specializations. Continued comparative work will also reveal whether the biophysical factors that alter activity after T-treatment converge with those active at baseline in *C. numenius*, whose long EODs are thought to represent a derived character state from an ancestral short EOD[49,50]. Morphological or physiological effects observed will be fascinating to consider in parallel with effects exerted by T on the electric organs of *B. brachyistius*, and those occurring throughout ontogeny in *Campylomormyrus*[20,27,28].

Putative molecular mechanisms driving CD shifts

Our results point to a fundamental puzzle: how can precise temporal coordination be maintained between anatomically and physiologically separate circuits in central and peripheral nervous systems? Given that T acts independently on the electric organ to elongate EODs and on MCA to shift CD timing, the submillisecond precision with which CD delays track reafferent input demands explanation. The solution may lie in shared or parallel regulatory mechanisms that ensure temporal coherence across these separately regulated systems.

Common molecular pathways may act on functionally analogous targets in electric organ and CD circuitry. Recent work has begun to illuminate the genomic basis for EOD waveform diversity[35,36], as well as the molecular cascade by which T elongates EODs in mormyrids[28]. T treatment upregulates expression of genes encoding numerous voltage-gated ion channels, as well as structural proteins that could alter electrocyte membrane properties and morphology[28]. Differential expression of ion channel genes is also linked with interspecific differences in EOD waveforms[52]. These transcriptional changes likely underpin the extensive biophysical remodeling observed after T: in addition to altered channel composition, electrocyte membranes undergo hypertrophy after T, and this increased surface area likely increases membrane capacitance to further contribute to action potential elongation[27,29]. These morphophysiological changes occur over several days to weeks, matching the time course observed for CD plasticity in *B. brachyistius.* Critically, many of the same ion channel families and structural proteins that are thought to determine electrocyte excitability and actional potential kinetics also regulate neuronal excitability in the brain[53–55]. We propose that T triggers parallel transcriptional programs in CD neurons that mirror those in electrocytes. A common molecular toolkit including voltage-gated ion channels, structural proteins, and their transcriptional regulators, could efficiently implement this coordinated plasticity on both central and peripheral targets.

In *B. brachyistius*, T alters CD timing in the absence of sensory feedback, suggesting plasticity arises exclusively from hormonal action in the brain[22]. Is this due to direct action on CD nuclei themselves, or indirect action via neuromodulators? T could act directly in CD nuclei by binding cytoplasmic androgen

receptors, or, after conversion to estradiol by aromatase, estrogen receptors—the latter being plausible due to high concentrations of aromatase in teleost brains[56]. Though a previous study found low androgen binding near mormyrid electromotor pathways outside breeding condition[30], androgen receptor expression increases in breeding condition and after T treatment in electromotor pathways of distantly related South American electric fish[57], suggesting that T can auto-induce expression of its own receptor[58,59]. Considering our data, bound receptors could alter gene expression in BCA (and possibly downstream nuclei) to drive these observed changes. The 2-week time courses of EOD-elongation and CD plasticity are consistent with this genomic mechanism, though rapid non-genomic actions may also be involved[60]. Alternatively, T could act indirectly through nearby neuromodulators such as serotonin, whose fibers pass through numerous electromotor and CD nuclei[61]. Though no study has yet tested for modulation of excitability by serotonin on these populations, this could provide an attractive central mediator for the plasticity we observe. Determining whether these shifts are autonomous to CD nuclei or if they require extrinsic neuromodulators is a critical next step.

Though sensory feedback is not necessary for hormonal CD plasticity, it could shape CD timing over longer developmental periods. Sensory feedback, altered gradually by developmental changes to electric organ morphology, could induce activity-dependent changes that fine-tune CD circuitry to elongated reafferent input. Alternatively, the same molecular factors that induce EOD elongation during development or evolution could circulate in the brain and regulate gene expression and physiology in CD neurons, as in T's parallel seasonal actions in electric organ and brain. As genomic and transcriptomic studies reveal candidate genes underlying hormonal EOD elongation in *Brienomyrus*[28] and EOD diversification in *Campylomormyrus*[51], it will be informative to extend these investigations into mormyrid brains—particularly to test whether the same ion channel genes and structural proteins that are differentially expressed in electric organs are also regulated in CD nuclei. Despite CD shifts being triggered by distinct proximate mechanisms across timescales, our data suggest that a common molecular program may ultimately be triggered to ensure reafferent input and CD timing are coordinated across the sensorimotor system.

Effects beyond the knollenorgan pathway

Temporal coordination between central and peripheral structures are particularly essential given the pervasive role of EOD waveform in mormyrid information processing. The EOD is not merely a communication signal; its temporal structure is a fundamental reference against which mormyrid nervous systems operate. CD pathways predict the timing of knollenorgan reafference (as demonstrated here), as well as reafference for active and passive electrolocation[2]. Sensory processing in higher-order centers integrates information about EOD timing to distinguish reafferent input from relevant features in the electrosensory scene[62,63]. Any change to EOD waveforms that was not precisely matched by corresponding shifts to these interconnected circuits would critically degrade sensorimotor function. These constraints may have driven the evolution of shared molecular regulatory systems to ensure that plasticity is inherently coordinated between peripheral and central structures.

Due to the interconnectivity of electromotor, electrosensory, and CD circuitry, changes to the timing of MCA activation should have wide-ranging consequences[2]. Though MCA receives input exclusively from BCA, axons of MCA neurons bifurcate into two separate pathways in addition to the CD inhibition circuit. One pathway is a recurrent inhibitory network that projects into the electromotor pathway to regulate EOD production[64,65]. The other is a separate CD that signals the timing of EOD production to sensory areas involved in active electrolocation, whose inputs arise from mormyromast electroreceptors[32] (not shown in Figure 1). Due to this shared circuitry, timing shifts at or upstream from MCA are likely to affect electromotor rhythm and sensory predictions for critical active sensing behaviors. This could further explain the convergence across various timescales of plasticity onto MCA:

to preserve a coherent sensorimotor phenotype within a constrained system, selection may have targeted this central hub to concurrently affect multiple pathways.

Conclusions

By maintaining the distinction between self and other, CDs underpin stable perception for all behaving animals. A taxonomy of CD effects has been described across the animal kingdom, spanning lower-order sensory filtration to higher-order roles in learning and planning complex movements[1]. Few studies have yet investigated how these CDs adapt to changes in the temporal structure of behavioral outputs. The mormyrid system offers an excellent starting point for revealing these mechanisms. By focusing on a CD consisting of a simple excitatory relay without complex synaptic integration or spontaneous activity, we isolated hormonal, developmental, and evolutionary changes in circuit physiology in the context of quantifiable shifts to reafference. We find that the same neural substrates support plasticity across diverse timescales. Other systems may also rely on a common, scalable solution acting on shared substrates to ensure coordinated circuit outputs over ontogenetic and evolutionary timescales. Alternatively, higher-order CD systems that mediate multisensory representations may need more degrees of freedom to update more complicated representations, in which case separate substrates may support plasticity across different timescales. Unraveling these mechanisms may yield therapeutic targets for when sensory predictions are decoupled from reafferent input: CD deficits have been demonstrated across sensory modalities in schizophrenia patients. These deficits are thought to underlie auditory hallucinations and “abnormal self-experiences” characteristic of the disorder[66,67], though the neural basis of these symptoms is still poorly understood due to our incomplete understanding of how sensory predictions are normally maintained. Additionally, hormonal imbalance at the critical periadolescent period may contribute to emergence of schizophrenia[68,69], though no direct connections of hormonal imbalance on CD dysfunction have yet been investigated. Further elucidation of how CD circuits support behavioral plasticity and hormonal sensitivity under nonpathological conditions will be invaluable for our understanding of the fundamental physiological requirements for temporal preservation in the brain.

Resource Availability

Lead Contact. Further information and requests for resources and reagents should be directed to and will be fulfilled by the Lead Contact, Bruce A. Carlson (carlson.bruce@wustl.edu).

Materials Availability. This study did not generate new unique reagents, strains, or lines.

Data and Code Availability. Raw, unprocessed data and all original code have been deposited at Zenodo and are publicly available as of the date of publication at 10.5281/zenodo.18839201.

Methods

Experimental Model and Subject Details. We used a total of 8 *Brienomyrus brachyistius* (7–8.5 cm in standard length), 8 *Campylomormyrus compressirostris* (10.5-15.5 cm in standard length), and 8 *Campylomormyrus numenius* (6.5-15.9 cm in standard length). For all species, we used fish of both sexes in non-reproductive state. Fish were purchased from Alikhan Tropical Fish. Fish were housed in groups with a 12 h: 12 h light/dark cycle, temperature of 25–29°C, pH of 6–7, and water conductivity of 175–225 μS/cm. Fish were fed live black worms or frozen blood worms four times per week. All procedures accorded with guidelines established by the National Institutes of Health and were approved by the Animal Care and Use Committee at Washington University in St. Louis.

Half of the *B. brachyistius* were testosterone-treated and the other half were vehicle-treated. *Campylomormyrus* species received no hormone treatment. All fish were used for simultaneous

recording of EOD and EODC, followed by field potential recordings from CD nuclei (CN, MRN, BCA, MCA, slem, and nELL) while recording the EODC.

Hormone Treatment of *B. brachyistius.* Methods were similar to a previous study[22]. A 40L tank was prepared for each treatment group, divided into four compartments with mesh panels, and filled with 30 L of aquarium water. For testosterone fish, 60 mg of solid 17a-methyltestosterone (Sigma-Aldrich) dissolved in 0.4 mL 95% ethanol was added to the testosterone tank once every two days over the course of 14 days. For vehicle fish, only 0.4 mL 95% ethanol was added to the vehicle tank on the same schedule as the testosterone treatment. Except for the treatment and separation with mesh panels, tank conditions were identical to normal housing.

EOD recording. EODs were recorded from freely swimming fish. In *B. brachyistius,* we recorded EODs immediately prior to the start of hormone treatment and at the end of hormone treatment, prior to electrophysiology. In *Campylomormyrus*, we recorded EODs immediately prior to electrophysiology. EODs were amplified 10 times, bandpass filtered (1 Hz–50 kHz) (BMA-200, CWE), digitized at a rate of 195 kHz (RP2.1, Tucker-Davis Technologies), and stored using custom software in MATLAB (The MathWorks). From the triphasic EOD waveform of *B. brachyistius*, we determined EOD onset as the point crossing 20% the amplitude of the first head-negative peak (often called peak 0) and EOD offset as the point crossing the last 2% deviation from the overall peak-to-peak amplitude. From the biphasic waveform of *C. compressirostris* and *C. numenius*, which lacks a peak 0, EOD onset and offset were determined as the point crossing the first and last 2% deviation from the peak-to-peak amplitude, respectively[20]. For all species, EOD duration was the period between EOD onset and offset.

EOD and EOD command recording. Recordings were performed immediately before field potential recording according to a previous study[22]. Fish were anesthetized in a solution of 300 mg/L MS-222 (Millipore Sigma) and placed on a plastic platform with lateral supports in a recording chamber filled with freshwater covering the entire body of the fish. To control for effects of temperature on electromotor output, we maintained the water temperature in our recording chamber by looping plastic tubing through the tank. The tubing connected to a pump in a bucket containing deionized water and a heater. By circulating warm water through the tubing, we heated the recording tank by conduction to maintain a constant temperature of 26.5-28.5 degrees C. Fish were restrained by lateral plastic pins, a plastic tube on the tail, and two folded paper towels on the dorsal skin surface. The EODC from spinal electromotor neurons (EMNs) was recorded with a pair of electrodes located within the plastic tube and oriented parallel to the fish's electric organ, amplified 1000x, and bandpass filtered (10 Hz to 5 kHz) (Model 1700, A-M Systems). While the EODC was recorded, EODs were recorded by separate electrodes, amplified 10 times, and band-pass filtered (1 Hz to 50 kHz) (BMA-200, CWE). These recordings were digitized at a rate of 1 MHz and saved (TDS 3014C, Tektronix).

The EODC was averaged across trials, and EOD traces were filtered by a 21st-order median filter whose time window was 0.02 ms and averaged across trials. EOD onset was determined as in the freely swimming EOD recordings. EODC onset was determined as the first negative peak in the averaged EMN trace. Delay to EOD onset was calculated as the time between EODC onset and EOD onset. Delay to EOD peak 1 from the EOD command was calculated as the sum of the delay to EOD onset and the delay between EOD onset and peak 1 recorded from freely swimming fish. We termed the delay from EOD command to EOD p1 "Reafferent Delay".

Field potential recordings from CD nuclei. Recording and analyses were similar to previous studies[22,34,64]. Recordings in *B. brachyistius* were performed after 14-16 days of treatment. Fish were anesthetized with a solution of 300 mg/L MS-222 and paralyzed with 0.1-0.12 mL of 3.0 mg/mL Flaxedil. Fish were transferred to a recording chamber filled with water heated to 26.5-28.5 degrees C

and positioned on a plastic platform, leaving the surface of the head above water level. During surgery, we maintained general anesthesia by respirating the fish with an aerated solution of 100 mg/ml MS-222 through a pipette tip placed in the mouth. For *Campylomormyrus*, we connected a hose made from heat shrink tubing to the pipette tip to provide respiration to the long tube-snout. For local anesthesia, we applied 0.2% lidocaine on the skin overlying the incision site and then made an incision to uncover the skull overlying the dorsal surface of the brain. Next, we glued a headpost to the skull before using a dental drill and forceps to remove a rectangular piece of skull covering the brain. Following surgery, we gently removed the glued headpost from the skull and rotated the platform 34 degrees to be coaxial with the approach angle of our recording electrode. After re-gluing the headpost to situate the fish in this position, we switched respiration to fresh water and allowed the fish to recover from anesthesia. We then placed a reference electrode on the nearby cerebellum. The EODC was recorded from EMNs and sent to a window discriminator for time stamping (SYS-121, World Precision Instruments).

Recording electrodes (Model 626000, A-M Systems) were pulled with a micropipette puller (Model P-97, Sutter Instrument), broken to 5–10μm internal tip diameter, and filled with 3 M NaCl solution. Recording electrodes were controlled by a motorized micromanipulator (MPC-200 with a ROE-200 controller, Sutter Instruments).

Spontaneous EODC triggered 20 ms or 40 ms recording sweeps in the brain as we searched for CD nuclei. We located CD nuclei based on proximity to surface landmarks on the brain (Figure 6A) and EODC-related field potentials, which they exhibit with characteristic waveforms and latencies relative to the EOD command (Figure 6B). To account for possible damage to axonal projections during recording, we recorded first from the end of the pathway, in nELL, and worked backwards through slem, MCA, BCA, MRN, then finally CN. Field potentials were amplified 1000x, bandpass filtered (10 Hz–5 kHz, Model 1700, A-M Systems), and, in most cases, digitized at a rate of 97.7 kHz (RX8, Tucker-Davis Technologies) and stored using custom software in MATLAB. In some cases, recordings were digitized at 500 kHz (TDS 3014C, Tektronix) and downsampled in MATLAB by a factor of 5 to 100kHz. In all cases, we averaged 16 traces to measure command-related timing at each nucleus.

Due to small size of nuclei and their varying depth in the brain, we attempted several sites before finding a suitable recording site. Once a characteristic waveform was detected, the electrode penetration site was continually moved in 50-200μm increments in the direction of increasing field potential amplitude, finally encircling the point of maximum amplitude. A single recording position with maximum amplitude was used to score the timing of a given nucleus. Brains of *Campylomormyrus* were larger than those of *Brienomyrus*, with more of the dorsal surface covered by the valvula cerebellum. Though CD nuclei of *Campylomormyrus* were typically found >1mm deeper than in *Brienomyrus*, their positions relative to surface landmarks along anteroposterior and mediolateral axes were similar to *Brienomyrus*, which facilitated localization of nuclei.

We measured onset and offset of field potentials as the first and last peaks in the waveform, respectively, relative to the first negative peak of the EODC. We defined peaks as local maxima/minima in the command-related potentials that scaled together in amplitude as the nucleus was approached. Because CD nuclei do not exhibit spontaneous activity in the absence of CD input from CN, this activity synchronized 1:1 with EOD command signals. Duration of field potentials was defined as the period between onset and offset. Criteria for scoring onset and offset peaks were based on observed patterns across fish and in corroboration with descriptions from the literature[17,31,33,34,70]. We developed a custom Matlab function to score timing, with parameters that captured the unique activity of each nucleus (detailed below). This enabled unsupervised

measurement for all treatment groups/species, wherein only nucleus ID needed to be input to reliably measure CD timing. This function detected peaks using the peakfinder function in MATLAB[71] which detects local maxima/minima separated from surrounding data by a given selectivity value and, if desired, crossing a specified threshold. Timing window, selectivity and threshold varied across nuclei due to varying peak numbers and relative amplitudes/polarities of peaks.

Command and Medullary Relay Nuclei (CN/MRN): CN and MRN are midline structures located near the ventral surface of the medulla[33]. MRN provides the only known source of direct descending input to drive electromotor neuron activity. CN is just ventral to MRN, and provides monosynaptic input to MRN, constituting the start of the electromotor pathway, and to BCA, constituting the start of the CD pathway. Field potential waveforms of CN and MRN typically consisted of two peaks. The first CN peak occurred around -2.2 ms (all times given relative to first negative peak of EODC), and the second peak occurs at roughly +0.5 ms. The first MRN peak occurs a couple hundred microseconds after CN p1 and the second peak occurs right around the EODC. Due to the proximity of CN and MRN, this second MRN peak near the EODC could often be detected at low amplitude near CN.

We obtained CN recordings in 23/24 fish. CN onset was determined as the point of absolute maximum or minimum in the voltage trace (for positive or negative peaks, respectively) between -3 and -0.5 ms. After peak 1, voltage usually overshot the baseline. In most cases it then returned into a rounded 2nd peak (17/23 fish), though in some cases (6/23 fish), this offset peak was less distinct and appeared as a flattening or inflection in the trace. Inspection of the derivative of the voltage trace of all fish revealed a distinct peak in this window that closely corresponded in time to both the clear voltage peaks and inflections. Thus, we expect that these inflections represent the same activity as the clear second peak and simply reflect variations between fish in current source density near CN. To determine offset for all cases, we detected the last prominent peak in the derivative trace between -0.15 ms and +2 ms, with a peak selectivity of ¼ of the range of the derivative trace. We then detected the next prominent local maximum or minimum in the derivative trace (for negative and positive derivative peaks, respectively). We defined offset as the time corresponding to the midpoint between the peak in the derivative trace and the subsequent maximum/minimum.

We obtained MRN recordings from 23/24 fish. MRN peaks were detected with selectivity of 1/8 the range of the voltage trace prior to +1ms. The first peak in this window was defined as MRN onset, and the last peak as offset.

Bulbar Command-Associated nucleus (BCA): BCA is located in the brainstem ~800μm lateral to the midline at the level of the lateral reticular nucleus[31]. Field potentials recorded from BCA consist of two peaks of the same polarity separated by about 2ms, with the first occurring about 2ms before the EODC.

We recorded BCA in 23/24 fish. BCA peaks were detected as local maxima/minima separated from surrounding data by ¼ of the range of the voltage trace prior to +1ms. The first peak was defined as BCA onset, and the last peak as offset.

Mesencephalic Command-Associated nucleus (MCA): MCA is located ~ 500um lateral to the midline, at the anterior edge of the valvular peduncle[31]. The field potential waveform typically consists of two elements which can be recorded in relative isolation to one another[34]. The first element consists of two peaks that occur around -1.2 ms and +1.5-2.2 ms relative to the EODC, which are attributed to presynaptic BCA axon terminals. The second element consists of two peaks which are often nested between the two peaks of the first element and separated by about 0.7ms, which are attributed to postsynaptic MCA neurons (see *Discussion* for further interpretation of field potentials). In T-treated fish and *C. numenius,* the overall waveform was elongated, and an additional peak was

observed in this window in many cases. Because the small size of MCA made it challenging to fully separate putative pre- and postsynaptic elements without using juxta- or intracellular recordings, we used a single recording site that maximally included all elements to score timing of MCA field potentials for a given fish.

We recorded MCA in 24/24 fish. MCA peaks were defined as maxima separated from surrounding data by 1/12 of the total range of the voltage trace. Onset was defined as the first detected peak and offset was the last peak within 5 ms of the first peak. This window size was used to exclude slower, longer-latency activity that did not scale in amplitude with activity recorded near MCA.

Sublemniscal nucleus (slem): slem is a subpopulation of the juxtalemniscal nucleus, just ventral to the lateral lemniscus at the level of nucleus praeeminentialis. All juxtalemniscal neurons receive their input from MCA. An excitatory subset of juxtalemniscal neurons provides CD input to the medial juxtalobar nucleus, as part of a related CD pathway for active electrolocation[32]. Slem, on the other hand, provides GABAergic inhibition to nELL. Field potentials in this region consist of 2 sharp peaks separated by ~1 ms, beginning close to the EODC (partial waveform shown in [70]). These peaks scaled uniformly in amplitude with one another and scaled distinctly from a background signal beginning around -1.8 ms and ending between +1.5-2 ms relative to the EODC, which reflected activity from the nearby paratrigeminal command-associated nucleus as part of another CD circuit for passive electrolocation[31].

We recorded slem in all 24/24 fish. Because slem peaks could be positive or negative based on electrode position, peak polarity was manually input by the scorer. Peaks were detected as maxima/minima separated from surrounding data by 1/5 of the total range of the voltage trace and exceeding a threshold of one standard deviation above or below the baseline. Similar to the elongated MCA waveform, slem waveforms in T-treated fish and *C. numenius* showed a prominent third peak with similar kinetics to the first two peaks. To distinguish this possible third peak from kinetically slower background activity unrelated to slem, we only included peaks separated by less than 1.3 ms from previous peaks. Further, we discarded any peaks detected after p2 whose width was more than 2x the average width of the first two peaks. In 2/24 fish, only one peak was detected due to a sharp drop past baseline after the first peak, leading subsequent maxima to not pass the threshold for detection. In these cases, we manually measured the magnitude of subsequent local maxima as putative peaks. If putative peaks were within 80% of p1 amplitude and met all other criteria for timing and kinetics listed above, they were included for analysis.

Nucleus of the electrosensory lateral line lobe (nELL): nELL is a thin, tubelike nucleus at the dorsolateral edge of the Electrosensory Lateral Line lobe (ELL). We identified nELL by its command-related potential, which consists of a single positive-negative peak occurring several ms after the EODC[17]. A second criterion for localizing nELL was the characteristic potentials evoked in nELL by electrosensory stimuli. We presented 0.2 ms bipolar square pulses and 30ms monopolar square pulses transverse to the body (right-side positive), of both normal and reversed polarity at an intensity of 73.6 mV/cm. Proximity to nELL was confirmed by short-latency (1.5-2ms) potentials evoked by bipolar square waves, by onset of reversed-polarity monopolar square waves, and by offset of normal-polarity monopolar square waves. The timing of CD- and electrosensory evoked potentials varies slightly along the length of the nucleus due to somatotopy of the projections, with rostral regions exhibiting shorter-latency potentials compared to caudal regions[17]. When recording from nELL, we attempted to record from the full extent of the nucleus and used the median recording site as the representative nELL potential.

We recorded from nELL in all 24/24 fish. The ELL surrounds nELL and elicits longer-latency CD-related potentials[62], which complicated detection of the single nELL peak from voltage alone. We

noted, however, that the sharp negative-going potential after the single nELL peak always corresponded to the absolute minimum in the derivative of the voltage trace. Thus, the peak of the nELL potential was identified as the local maximum in the voltage trace occurring directly before the time corresponding to this absolute minimum in the derivative trace.

Statistical Analysis

Analyses were performed in Excel and Matlab. We compared mean differences in EOD duration within groups before and after hormone/vehicle treatment using paired Student's *T*-tests. We used Welch's t-tests, which assume unequal variance of groups, to compare between treatment groups or across species. These comparisons included CD inhibition onset/duration, EOD duration, onset timing of each nucleus relative to EODC p0, and duration of field potentials at each nucleus (offset – onset timing). Differences were deemed statistically significant with $p < 0.05$, and effect size was calculated using Cohen's *d*.

We computed standard linear regressions of reafferent delay (delay from EODC p0 to EOD p1) vs. CD nucleus onset and reafferent delay vs. CD nucleus duration using Excel. When comparing superlong-EOD *C. numenius* to other *C. numenius*, we computed Z scores of onset and duration of each nucleus and computed P(onset < -Z or onset > Z) as the area under the normal distribution curve.

Figure Legends

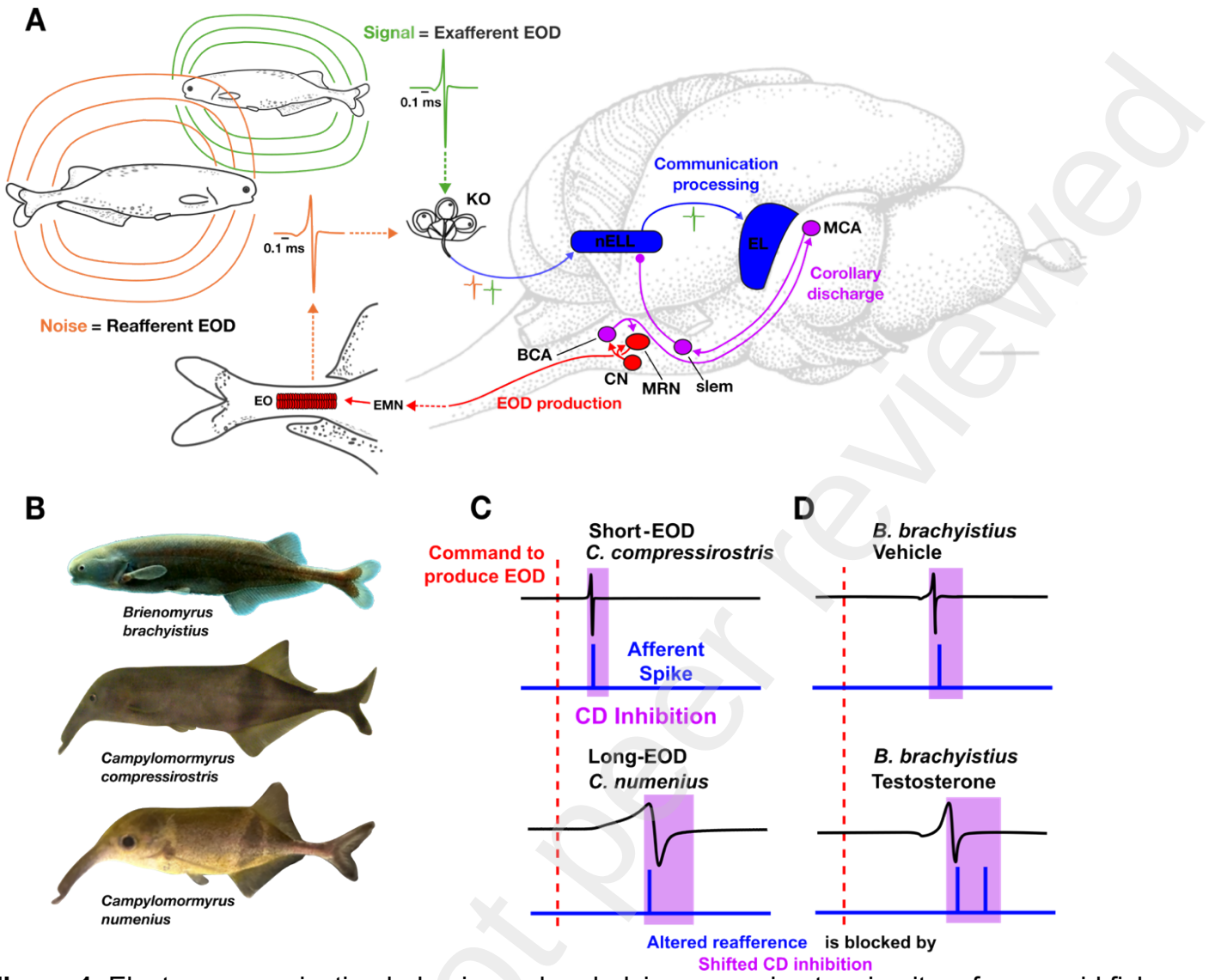

Figure 1. Electrocommunication behavior and underlying sensorimotor circuitry of mormyrid fish

(A) Diagram of electrocommunication behavior and neuroanatomy of electromotor (red), corollary discharge (purple), and electrosensory (blue) pathways in mormyrids. Excitatory connections are indicated by arrows, whereas inhibitory connections are indicated by punctate terminals. EODs are initiated by the command nucleus (CN). This signal is sent to a medullary relay nucleus (MRN). MRN excites electromotor neurons (EMN) in the spinal cord, which activate electrocytes in the electric organ (EO) to produce a single EOD. Knollenorgan (KO) electroreceptors on the skin respond to reafferent (orange) and exafferent (green) EODs, and their primary afferents terminate in the nucleus of the electrosensory lateral line lobe (nELL), which projects to the exterolateral nucleus (EL) for further processing. A copy of the CN command is sent to nELL via three CD nuclei: the bulbar command-associated nucleus (BCA), the mesencephalic command-associated nucleus (MCA), and finally the GABAergic sublemniscal nucleus (slem), which inhibits nELL to block responses to reafferent EODs. Scale bar on brain = 1 mm. (B) Photographs of mormyrid species used in this study. (C) Illustration of representative data from [21], comparing timing of EOD production, associated afferent spike and CD inhibition relative to the command to produce EODs for short-EOD *C. compressirostris* (top) and long-EOD *C. numenius* (bottom). (D) Illustration of representative data from [22] depicting same events as in (C) but comparing relative timing of a vehicle- and testosterone-treated *B. brachyistius*.

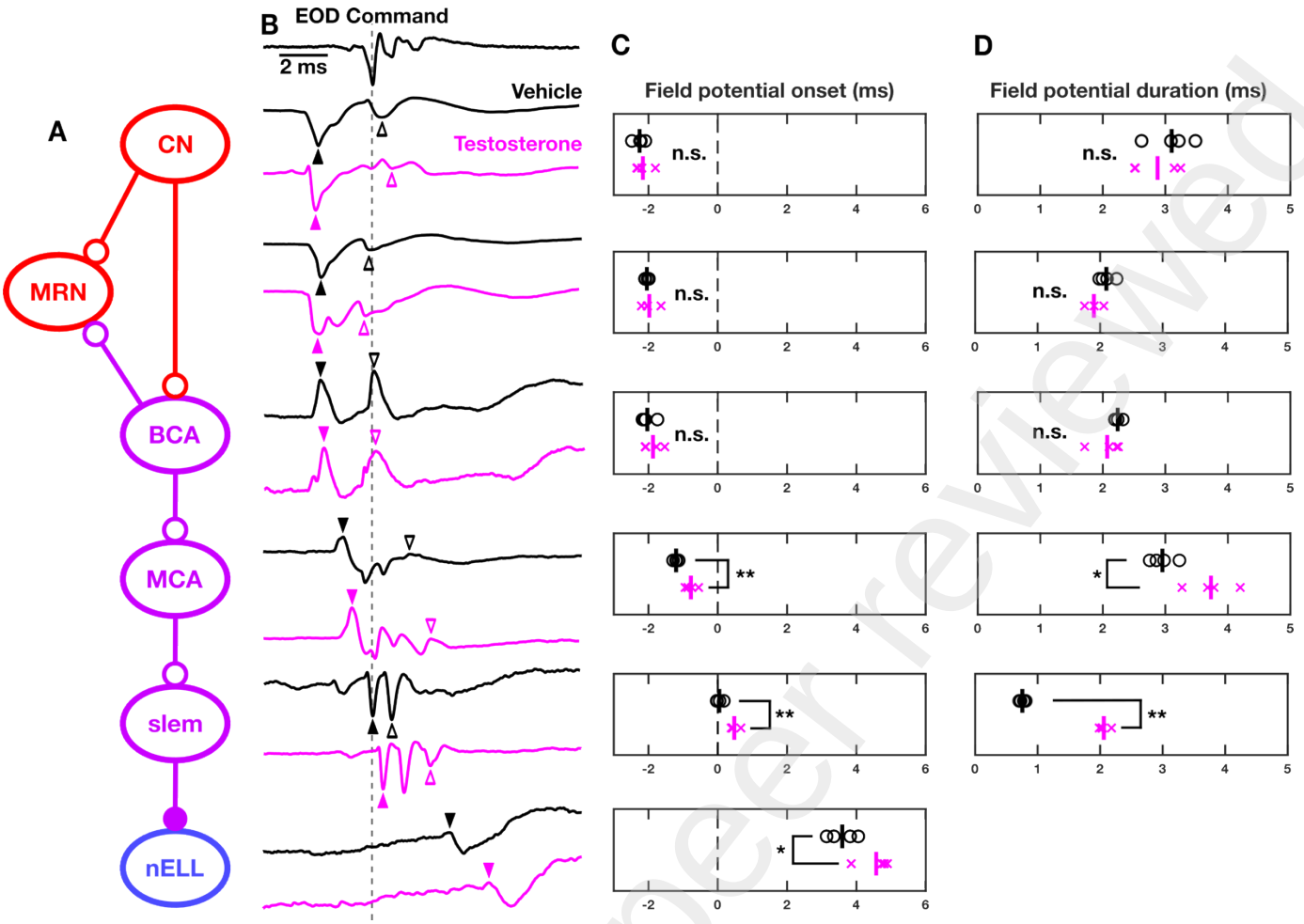

Figure 2: Corollary discharge timing is shifted by testosterone treatment
(A) Diagram of CD pathway with electromotor input and electrosensory output. (B) Command-related field potentials of CD nuclei from representative V- and T-treated fish (average of 16 traces). Each nucleus fires potentials at a characteristic delay relative to the EODC, the onset of which is denoted by filled arrowheads. T treatment induces delayed conduction of CD signal starting at MCA, which propagates through to slem and nELL. MCA and slem waveforms of T-treated fish also contain an additional peak (open arrowheads), which could underlie elongated CD inhibition in nELL. The first spike in the 3-spike EODC is a universal timing reference across fish (grey vertical line), and potentials are scaled to arbitrary height. (C) Summary data of CD nucleus onset timing relative to the EODC, for vehicle and T-treated fish (n=4 each). (D) Summary data of field potential duration for nuclei whose waveforms contain multiple peaks, measured as time from onset to offset. n.s.: not significant; *: $p < 0.05$; **: $p < 0.005$, Welch's T-test.

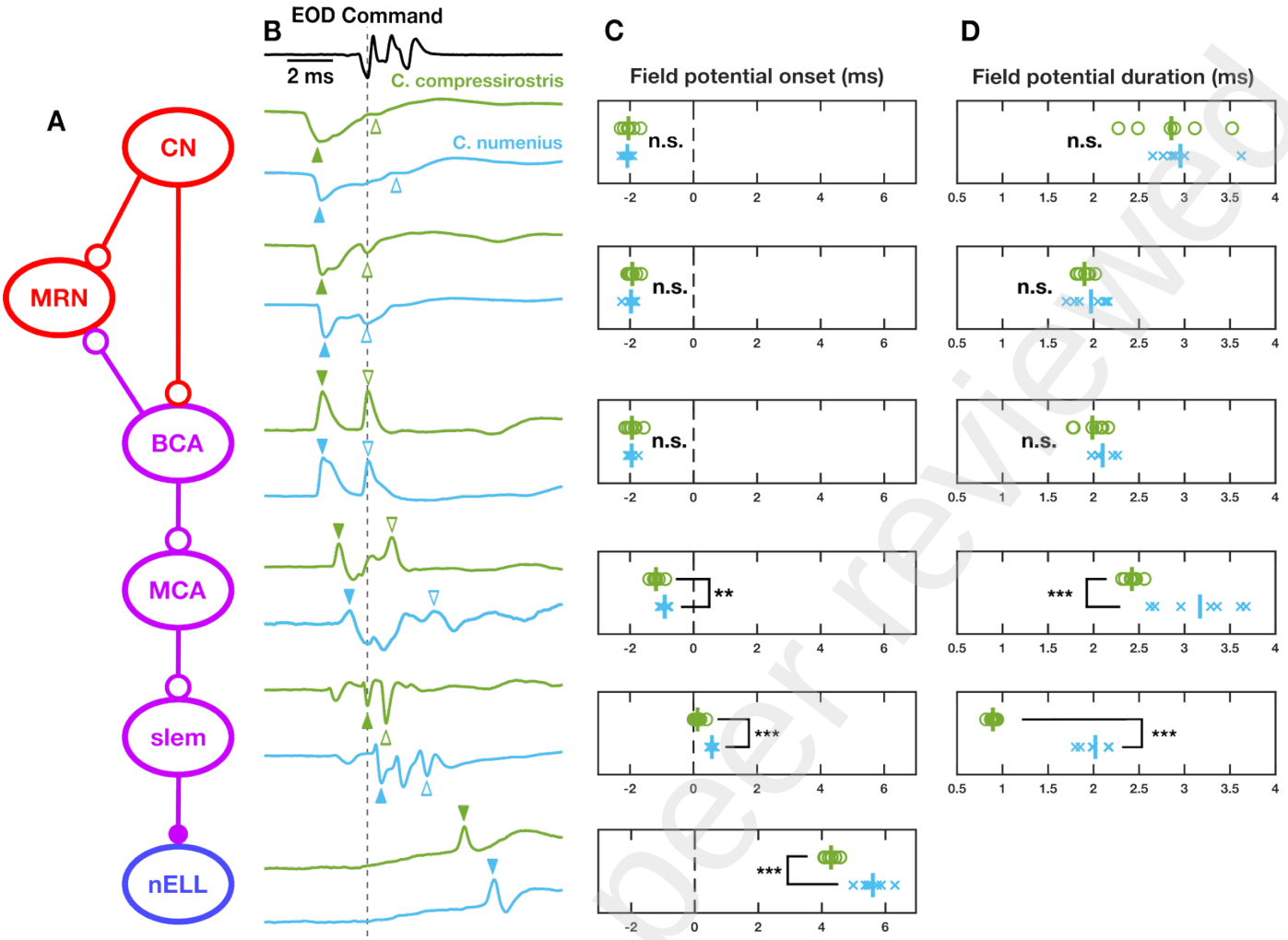

Figure 3: Neural substrates of species differences in corollary discharge timing
(A) Diagram of CD pathway with electromotor input and electrosensory output. (B) Command-related field potentials of CD nuclei from a representative short-EOD *C. compressirostris* (green) and long-EOD *C. numenius* (cyan, average of 16 traces). Compared to short-EOD fish, long-EOD fish show delayed activity starting at MCA onset, which carries through to slem and nELL. MCA and slem waveforms are also elongated in long-EOD fish compared to short-EOD fish, which could underlie elongated CD inhibition in nELL. Potentials are scaled to arbitrary height. (C) Summary data of CD nucleus onset timing relative to the EODC, for *C. compressirostris* (n=8) and *C. numenius* (n=7). (D) Summary data of field potential duration for nuclei whose waveforms contain multiple peaks, measured as time from onset to offset. n.s.: not significant; ** : $p < 0.005$; *** : $p < 0.00005$, Welch's T-test.

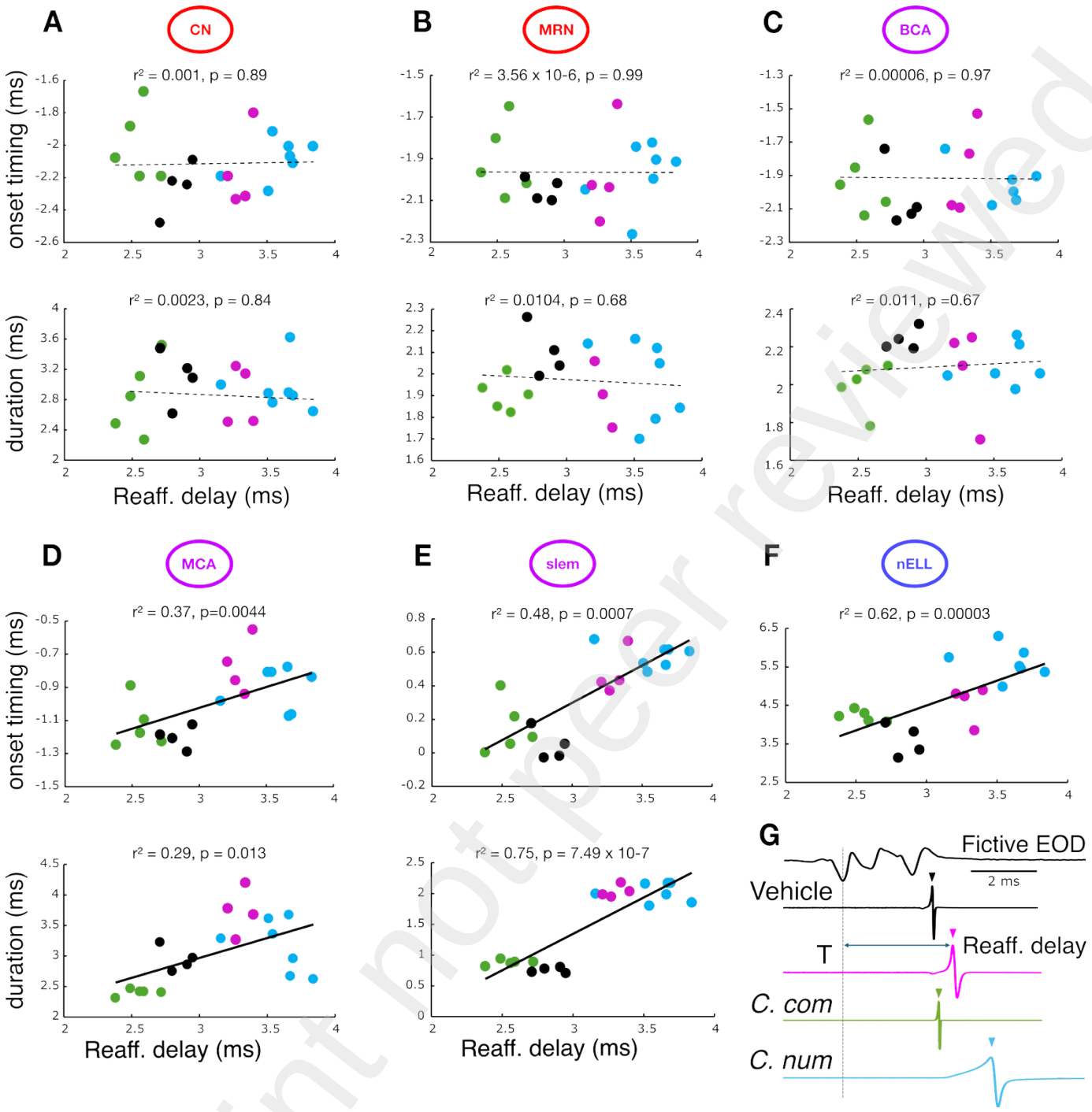

Figure 4: Over both seasonal and evolutionary timescales, CD onset timing and duration correlate with reafference downstream from BCA

(A-F) Plot of field potential onset timing (top) or duration (bottom) against reafferent delay (x axis) for the six nuclei measured. Each subfigure shows data from the indicated nucleus, presented in order of CD signal procession (CN, MRN, BCA, MCA, slem, nELL). As nELL field potentials only contained one peak, only onset timing is shown in (F). Points represent individual fish, color-coded by species/treatment group as indicated in (G). Regression lines were determined using standard regression. Solid lines indicate significant correlations. (G) Comparison of latency between the EODC and EOD peak 1 (termed reafferent delay) for representative vehicle and T-treated *B. brachyistius*, *C. compressirostris,* and *C. numenius*.

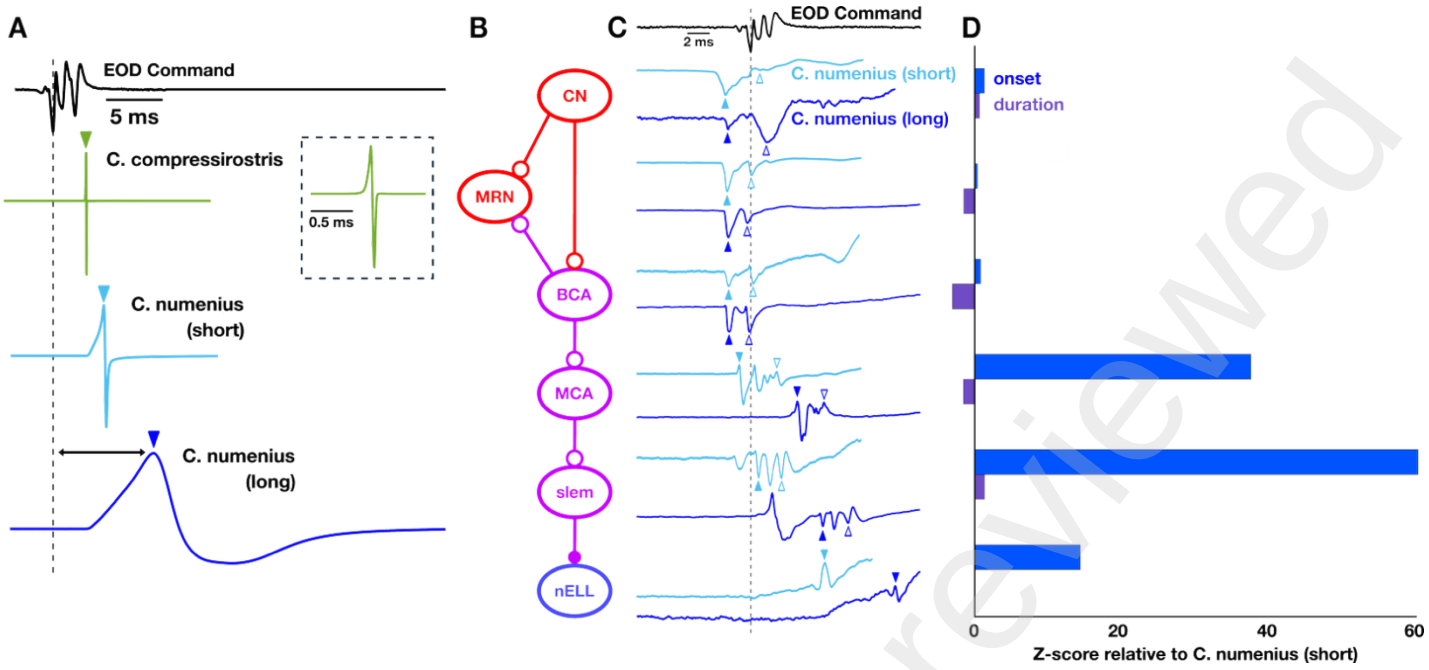

Figure 5: Corollary discharge shifts are accentuated in a superlong-EOD *C. numenius* at the same loci
where species differences and hormonal plasticity occur
(A) Comparison of reafferent delay between representative *C. compressirostris, C. numenius* (short), and *C. numenius* (long). (B) Diagram of CD pathway with electromotor input and electrosensory output. (C) Command-related field potentials of CD nuclei in another representative *C. numenius* (cyan, from dataset shown in Figure 3) and superlong-EOD *C. numenius* (royal blue, average of 16 traces). Compared to shorter-EOD *C. numenius*, this superlong-EOD fish shows further delays starting at MCA onset, which carries through to slem and nELL. MCA and slem waveforms show species-typical durations in superlong-EOD fish. Potentials are scaled to arbitrary height. (D) Z-score of onset timing (blue) and field potential duration (purple) for each nucleus recorded from superlong-EOD *C. numenius*, computed relative to the mean and standard deviation of conspecific *C. numenius.*

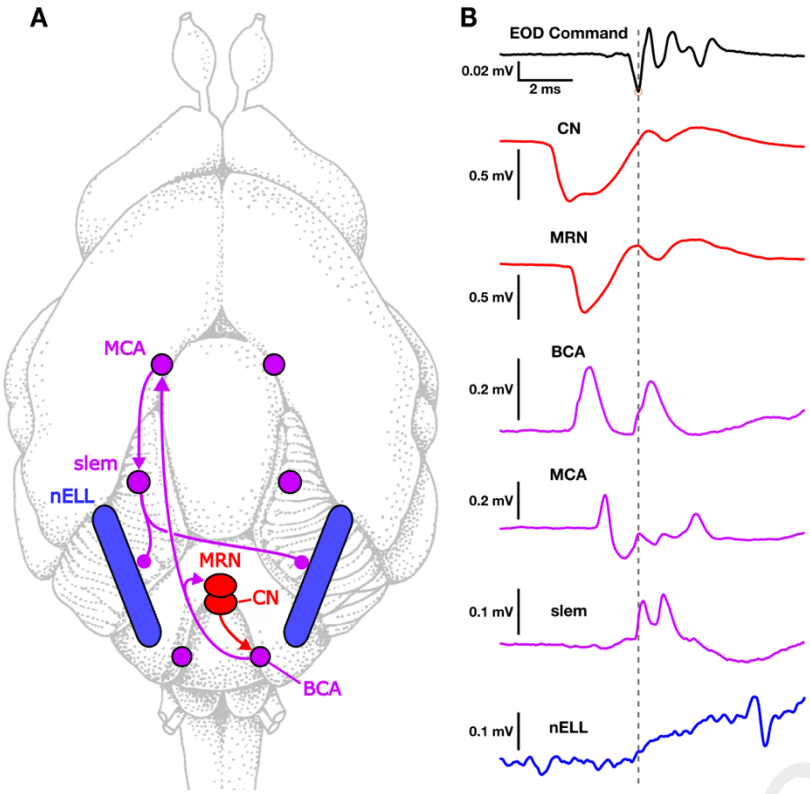

Figure 6: Anatomical position and field potentials of sensorimotor circuitry of mormyrid fish (A) Dorsal view of brain surface of *Brienomyrus brachyistius* with relevant electromotor (red), corollary discharge (purple), and electrosensory (blue) nuclei labeled. (B) Typical EODC-related field potentials from each nucleus recorded relative to fictive EOD and color-coded by pathway.

Supplemental Figures

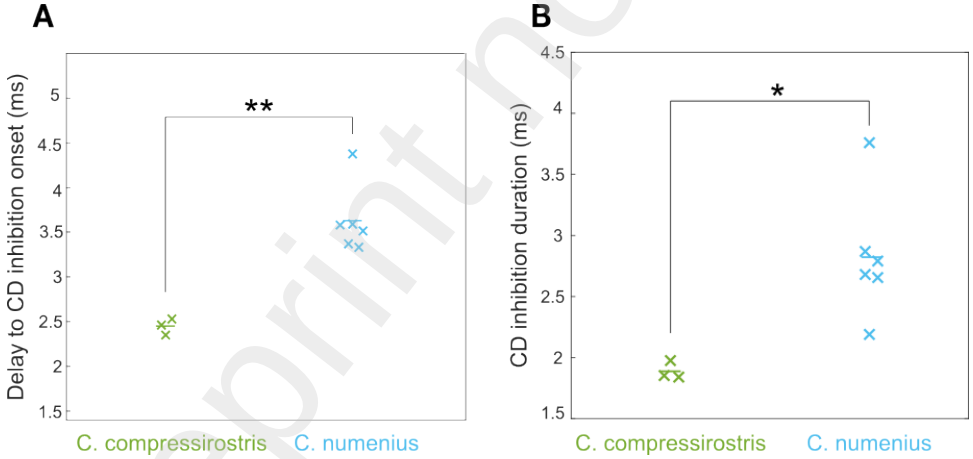

Figure S1: CD inhibition is delayed and elongated in long-EOD *C. numenius* compared to short-EOD *C. compressirostris*. (A) Comparison of CD inhibition onset timing between short-EOD *C. compressirostris* (n=3) and long-EOD *C. numenius* (n=6). (B) Comparison of CD inhibition duration between *C. compressirostris* and *C. numenius.* Data courtesy of Dr. Matasaburo Fukutomi. For details on CD inhibition recording, see [21]. * : $p < 0.01$; ** : $p < 0.001$ Welch's *t*-test.

References

1. Crapse, T. B. & Sommer, M. A. Corollary discharge across the animal kingdom. *Nat. Rev. Neurosci.* **9**, 587–600 (2008).
2. Fukutomi, M. & Carlson, B. A. A History of Corollary Discharge: Contributions of Mormyrid Weakly Electric Fish. *Front. Integr. Neurosci.* **14**, (2020).
3. Sperry, R. W. Neural basis of the spontaneous optokinetic response produced by visual inversion. *J. Comp. Physiol. Psychol.* **43**, 482–489 (1950).
4. von Holst, E. & Mittelstaedt, H. Das Reafferenzprinzip. *Naturwissenschaften* **37**, 464–476 (1950).
5. Poulet, J. F. A. & Hedwig, B. The Cellular Basis of a Corollary Discharge. *Science* **311**, 518–522 (2006).
6. Vélez, A., Kohashi, T., Lu, A. & Carlson, B. A. The cellular and circuit basis for evolutionary change in sensory perception in mormyrid fishes. *Sci. Rep.* **7**, 3783 (2017).
7. Podos, J. Correlated evolution of morphology and vocal signal structure in Darwin's finches. *Nature* **409**, 185–188 (2001).
8. Katz, P. S. Neural mechanisms underlying the evolvability of behaviour. *Philos. Trans. R. Soc. B Biol. Sci.* **366**, 2086–2099 (2011).
9. Otte, D. Evolution of Cricket Songs. *J. Orthoptera Res.* 25–49 (1992) doi:10.2307/3503559.
10. Small, T. W., Brenowitz, E. A., Wojtenek, W. & Moore, I. T. Testosterone mediates seasonal growth of the song control nuclei in a tropical bird. *Brain. Behav. Evol.* **86**, 110–121 (2015).
11. Tramontin, A. D., Hartman, V. N. & Brenowitz, E. A. Breeding Conditions Induce Rapid and Sequential Growth in Adult Avian Song Control Circuits: A Model of Seasonal Plasticity in the Brain. *J. Neurosci.* **20**, 854–861 (2000).
12. Hopkins, C. D. Temporal structure of non-propagated electric communication signals. *Brain. Behav. Evol.* **28**, 43–59 (1986).
13. Hopkins, C. D. & Bass, A. H. Temporal Coding of Species Recognition Signals in An Electric Fish. *Science* **212**, 85–87 (1981).

14. Carlson, B. A. Electric signaling behavior and the mechanisms of electric organ discharge production in mormyrid fish. *J. Physiol.-Paris* **96**, 405–419 (2002).
15. Xu-Friedman, M. A. & Hopkins, C. D. Central mechanisms of temporal analysis in the knollenorgan pathway of mormyrid electric fish. *J. Exp. Biol.* **202**, 1311–1318 (1999).
16. Baker, C. A., Kohashi, T., Lyons-Warren, A. M., Ma, X. & Carlson, B. A. Multiplexed temporal coding of electric communication signals in mormyrid fishes. *J. Exp. Biol.* **216**, 2365–2379 (2013).
17. Bell, C. & Grant, K. Corollary discharge inhibition and preservation of temporal information in a sensory nucleus of mormyrid electric fish. *J. Neurosci.* **9**, 1029–1044 (1989).
18. Mugnaini, E. & Maler, L. Cytology and immunocytochemistry of the nucleus of the lateral line lobe in the electric fish Gnathonemus petersii (mormyridae): Evidence suggesting that GABAergic synapses mediate an inhibitory corollary discharge. *Synapse* **1**, 32–56 (1987).
19. Hopkins, C. D. Design features for electric communication. *J. Exp. Biol.* **202**, 1217–1228 (1999).
20. Paul, C. *et al.* Comparative histology of the adult electric organ among four species of the genus Campylomormyrus (Teleostei: Mormyridae). *J. Comp. Physiol. A* **201**, 357–374 (2015).
21. Fukutomi, M. & Carlson, B. A. Signal Diversification Is Associated with Corollary Discharge Evolution in Weakly Electric Fish. *J. Neurosci.* **40**, 6345–6356 (2020).
22. Fukutomi, M. & Carlson, B. A. Hormonal coordination of motor output and internal prediction of sensory consequences in an electric fish. *Curr. Biol.* **33**, 3350-3359.e4 (2023).
23. Fukutomi, M. & Carlson, B. A. Coordinated changes in sensorimotor integration underlie behavioral change through evolution and plasticity: A case study in weakly electric mormyrid fish. *Sci. Prog.* **107**, 00368504241269438 (2024).
24. Bell, C. C. Sensory coding and corollary discharge effects in mormyrid electric fish. *J. Exp. Biol.* **146**, 229–253 (1989).
25. Bass, A. H. & Hopkins, C. D. Hormonal control of sex differences in the electric organ discharge (EOD) of mormyrid fishes. *J. Comp. Physiol. A* **156**, 587–604 (1985).

26. Kirschbaum, F. Reproduction and development of the weakly electric fish, Pollimyrus isidori (Mormyridae, Teleostei) in captivity. *Environ. Biol. Fishes* **20**, 11–31 (1987).
27. Freedman, E. G., Olyarchuk, J., Marchaterre, M. A. & Bass, A. H. A temporal analysis of testosterone-induced changes in electric organs and electric organ discharges of mormyrid fishes. *J. Neurobiol.* **20**, 619–634 (1989).
28. Losilla, M. & Gallant, J. R. Gene expression correlates and mechanistic insights into electric organ discharge duration changes in mormyrid electric fish. *J. Exp. Biol.* **228**, jeb249548 (2025).
29. Bass, A. H. & Volman, S. F. From behavior to membranes: testosterone-induced changes in action potential duration in electric organs. *Proc. Natl. Acad. Sci.* **84**, 9295–9298 (1987).
30. Bass, A. H., Segil, N. & Kelley, D. B. Androgen binding in the brain and electric organ of a mormyrid fish. *J. Comp. Physiol. A* **159**, 535–544 (1986).
31. Bell, C. C., Libouban, S. & Szabo, T. Pathways of the electric organ discharge command and its corollary discharges in mormyrid fish. *J. Comp. Neurol.* **216**, 327–338 (1983).
32. Bell, C. & von der Emde, G. Electric organ corollary discharge pathways in mormyrid fish. *J. Comp. Physiol. A* **177**, 463–479 (1995).
33. Grant, K., Emde, G. V. D., Sena, L. G. & Mohr, C. Neural command of electromotor output in mormyrids. *J. Exp. Biol.* **202**, 1399–1407 (1999).
34. Bell, C., Dunn, K., Hall, C. & Caputi, A. Electric organ corollary discharge pathways in mormyrid fish. *J. Comp. Physiol. A* **177**, 449–462 (1995).
35. Friedman, M. A. & Hopkins, C. D. Neural Substrates for Species Recognition in the Time-Coding Electrosensory Pathway of Mormyrid Electric Fish. *J. Neurosci.* **18**, 1171–1185 (1998).
36. Lyons-Warren, A. M., Kohashi, T., Mennerick, S. & Carlson, B. A. Detection of submillisecond spike timing differences based on delay-line anticoincidence detection. *J. Neurophysiol.* **110**, 2295–2311 (2013).
37. Carr, C. E. & Konishi, M. Axonal delay lines for time measurement in the owl's brainstem. *Proc. Natl. Acad. Sci.* **85**, 8311–8315 (1988).

38. Seidl, A. H. Regulation of Conduction Time along Axons. *Neuroscience* **0**, 126–134 (2014).
39. Kurz, E. M., Sengelaub, D. R. & Arnold, A. P. Androgens Regulate the Dendritic Length of Mammalian Motoneurons in Adulthood. *Science* **232**, 395–398 (1986).
40. Fargo, K. N., Galbiati, M., Foecking, E. M., Poletti, A. & Jones, K. J. Androgen regulation of axon growth and neurite extension in motoneurons. *Horm. Behav.* **53**, 716–728 (2008).
41. Hursh, J. B. Conduction velocity and diameter of nerve fibers. *Am. J. Physiol.-Leg. Content* **127**, 131–139 (1939).
42. Costa, A. R., Pinto-Costa, R., Sousa, S. C. & Sousa, M. M. The Regulation of Axon Diameter: From Axonal Circumferential Contractility to Activity-Dependent Axon Swelling. *Front. Mol. Neurosci.* **11**, 319 (2018).
43. Ford, M. C. *et al.* Tuning of Ranvier node and internode properties in myelinated axons to adjust action potential timing. *Nat. Commun.* **6**, 8073 (2015).
44. Waxman, S. G., Pappas, G. D. & Bennett, M. V. L. MORPHOLOGICAL CORRELATES OF FUNCTIONAL DIFFERENTIATION OF NODES OF RANVIER ALONG SINGLE FIBERS IN THE NEUROGENIC ELECTRIC ORGAN OF THE KNIFE FISH STERNARCHUS. *J. Cell Biol.* **53**, 210–224 (1972).
45. Waxman, S. G. Axon-glia interactions: Building a smart nerve fiber. *Curr. Biol.* **7**, R406–R410 (1997).
46. Zakon, H. H. The effects of steroid hormones on electrical activity of excitable cells. *Trends Neurosci.* **21**, 202–207 (1998).
47. Nudler, S. I., Pagani, M. R., Urbano, F. J., McEnery, M. W. & Uchitel, O. D. Testosterone modulates Ca(v2.2) calcium channels' functional expression at rat levator ani neuromuscular junction. *Neuroscience* **134**, 817–826 (2005).
48. Bean, B. P. The action potential in mammalian central neurons. *Nat. Rev. Neurosci.* **8**, 451–465 (2007).

921 49. Canitz, J., Kirschbaum, F. & Tiedemann, R. Transcriptome-wide single nucleotide polymorphisms
922 related to electric organ discharge differentiation among African weakly electric fish species. *PloS*
923 *One* **15**, e0240812 (2020).
924 50. Tiedemann, R., Feulner, P. G. D. & Kirschbaum, F. Electric Organ Discharge Divergence
925 Promotes Ecological Speciation in Sympatrically Occurring African Weakly Electric Fish
926 (Campylomormyrus). in *Evolution in Action: Case studies in Adaptive Radiation, Speciation and*
927 *the Origin of Biodiversity* (ed. Glaubrecht, M.) 307–321 (Springer, Berlin, Heidelberg, 2010).
928 doi:10.1007/978-3-642-12425-9_15.
929 51. Paul, C., Kirschbaum, F., Mamonekene, V. & Tiedemann, R. Evidence for Non-neutral Evolution
930 in a Sodium Channel Gene in African Weakly Electric Fish (Campylomormyrus, Mormyridae). *J.*
931 *Mol. Evol.* **83**, 61–77 (2016).
932 52. Losilla, M., Luecke, D. M. & Gallant, J. R. The transcriptional correlates of divergent electric organ
933 discharges in Paramormyrops electric fish. *BMC Evol. Biol.* **20**, 6 (2020).
934 53. Rudy, B. & McBain, C. J. Kv3 channels: voltage-gated K+ channels designed for high-frequency
935 repetitive firing. *Trends Neurosci.* **24**, 517–526 (2001).
936 54. Swapna, I. *et al.* Electrostatic Tuning of a Potassium Channel in Electric Fish. *Curr. Biol.* **28**, 2094-
937 2102.e5 (2018).
938 55. Zakon, H. H., Lu, Y., Zwickl, D. J. & Hillis, D. M. Sodium channel genes and the evolution of
939 diversity in communication signals of electric fishes: Convergent molecular evolution. *Proc. Natl.*
940 *Acad. Sci.* **103**, 3675–3680 (2006).
941 56. Forlano, P. M., Deitcher, D. L., Myers, D. A. & Bass, A. H. Anatomical Distribution and Cellular
942 Basis for High Levels of Aromatase Activity in the Brain of Teleost Fish: Aromatase Enzyme and
943 mRNA Expression Identify Glia as Source. *J. Neurosci.* **21**, 8943–8955 (2001).
944 57. Pouso, P., Quintana, L., Bolatto, C. & Silva, A. C. Brain androgen receptor expression correlates
945 with seasonal changes in the behavior of a weakly electric fish, *Brachyhypopomus gauderio*.
946 *Horm. Behav.* **58**, 729–736 (2010).

947 58. Aubele, T. & Kritzer, M. F. Androgen Influence on Prefrontal Dopamine Systems in Adult Male
948 Rats: Localization of Cognate Intracellular Receptors in Medial Prefrontal Projections to the
949 Ventral Tegmental Area and Effects of Gonadectomy and Hormone Replacement on Glutamate-
950 Stimulated Extracellular Dopamine Level. *Cereb. Cortex N. Y. NY* **22**, 1799–1812 (2012).
951 59. Bagamasbad, P. & Denver, R. J. Mechanisms and significance of nuclear receptor auto- and
952 cross-regulation. *Gen. Comp. Endocrinol.* **170**, 3–17 (2011).
953 60. Foradori, C. D., Weiser, M. J. & Handa, R. J. Non-genomic Actions of Androgens. *Front.*
954 *Neuroendocrinol.* **29**, 169–181 (2008).
955 61. Grant, K., Clausse, S., Libouban, S. & Szabo, T. Serotoninergic neurons in the mormyrid brain
956 and their projection to the preelectromotor and primary electrosensory centers:
957 Immunohistochemical study. *J. Comp. Neurol.* **281**, 114–128 (1989).
958 62. Bell, C. C., Grant, K. & Serrier, J. Sensory processing and corollary discharge effects in the
959 mormyromast regions of the mormyrid electrosensory lobe. I. Field potentials, cellular activity in
960 associated structures. *J. Neurophysiol.* **68**, 843–858 (1992).
961 63. Kennedy, A. *et al.* A temporal basis for predicting the sensory consequences of motor commands
962 in an electric fish. *Nat. Neurosci.* **17**, 416–422 (2014).
963 64. Carlson, B. A. Neuroanatomy of the mormyrid electromotor control system. *J. Comp. Neurol.* **454**,
964 440–455 (2002).
965 65. Carlson, B. A. & Hopkins, C. D. Central control of electric signaling behavior in the mormyrid
966 Brienomyrus brachyistius: segregation of behavior-specific inputs and the role of modifiable
967 recurrent inhibition. *J. Exp. Biol.* **207**, 1073–1084 (2004).
968 66. Ford, J. M. & Mathalon, D. H. Electrophysiological evidence of corollary discharge dysfunction in
969 schizophrenia during talking and thinking. *J. Psychiatr. Res.* **38**, 37–46 (2004).
970 67. Beño-Ruiz-de-la-Sierra, R. M. *et al.* Corollary Discharge Dysfunction as a Possible Substrate of
971 Anomalous Self-experiences in Schizophrenia. *Schizophr. Bull.* **50**, 1137–1146 (2023).

68. Brown, J. S. Association of Increased Prenatal Estrogen With Risk Factors for Schizophrenia. *Schizophr. Bull.* **37**, 946–949 (2011).
69. Markham, J. A. Sex steroids and schizophrenia. *Rev. Endocr. Metab. Disord.* **13**, 187–207 (2012).
70. von der Emde, G. & Bell, C. C. Nucleus preeminentialis of mormyrid fish, a center for recurrent electrosensory feedback. I. Electrosensory and corollary discharge responses. *J. Neurophysiol.* **76**, 1581–1596 (1996).
71. peakfinder(x0, sel, thresh, extrema, includeEndpoints, interpolate). https://www.mathworks.com/matlabcentral/fileexchange/25500-peakfinder-x0-sel-thresh-extrema-includeendpoints-interpolate (2025).